photonics

MDPI

Article

The Influence of On-Orbit Micro-Vibration on Space Gravitational Wave Detection

Zhiwei Chen [1,2], Chao Fang [1,*], Zhenpeng Wang [1,2], Changxiang Yan [1] and Zhi Wang [1,3,*]

[1] Changchun Institute of Optics, Fine Mechanics and Physics, Chinese Academy of Sciences, Changchun 130033, China; chenzhiwei19@mails.ucas.ac.cn (Z.C.); wangzhenpeng20@mails.ucas.ac.cn (Z.W.); yancx@ciomp.ac.cn (C.Y.)
[2] University of Chinese Academy of Sciences, Beijing 100049, China
[3] School of Fundamental Physics and Mathematical Sciences, Hangzhou Institute for Advanced Study, UCAS, Hangzhou 310024, China
* Correspondence: fangchao@ciomp.ac.cn (C.F.); wangzhi@ciomp.ac.cn (Z.W.)

Abstract: Large-aperture space telescopes have played an important role in space gravitational wave detection missions. Overcoming the influence of the space environment on interstellar laser distance measurement and realistic high-concentration laser distance measurement is one of the topics that LISA and Taiji are working hard on. It includes solar temperature, spatial stress relief, pointing shake and tilt, etc. However, when considering the impact of vibration on the telescope, both LISA and Taiji only consider the resonance impact of vibration on structural parts, which greatly ignores the impact of high-frequency micro-vibration on space ranging. This paper first considers space gravitational wave detection. Then, we establish the heterodyne interference model and demodulation algorithm of the optical phase-locked loop, and then introduce the vibration component for theoretical analysis. The results show that, although the resonance effect of low-frequency vibration on the system structure is avoided in space gravitational wave detection, the influence of high-frequency micro-vibration on heterodyne interference cannot be ignored. At the same time, we quantitatively analyze the influence efficiency of amplitude and frequency; in the premise of small amplitudes, the influence of vibration frequency is related to the frequency of the heterodyne signal, which has important guiding significance in engineering.

Keywords: micro-vibration; telescope; phase measurement; gravitational waves; Taiji

check for updates

Citation: Chen, Z.; Fang, C.; Wang, Z.; Yan, C.; Wang, Z. The Influence of On-Orbit Micro-Vibration on Space Gravitational Wave Detection. *Photonics* **2023**, *10*, 908. https://doi.org/10.3390/photonics10080908

Received: 16 June 2023
Revised: 24 July 2023
Accepted: 27 July 2023
Published: 7 August 2023

Copyright: © 2023 by the authors. Licensee MDPI, Basel, Switzerland. This article is an open access article distributed under the terms and conditions of the Creative Commons Attribution (CC BY) license (https://creativecommons.org/licenses/by/4.0/).

1. Introduction

Gravitational waves are a peculiar physical phenomenon predicted by Einstein's general theory of relativity, which propagate in the form of waves in the gravitational field. Gravitational wave detection is an important research topic in the field of modern astronomy and physics. The most famous and successful ground-based gravitational wave detector is LIGO (Laser Interferometer Gravitational Wave Observatory), which consists of two observatories located in the United States: Hanford, Washington, and Livingston, Louisiana. Each observatory has two interfering arms with a length of 4 km. In addition, the European Gravitational Wave Observatory Virgo is also a ground-based gravitational wave detector located in Pisa, Italy, which has three interference arms with a length of 3 km [1]. However, due to the interference of ground noise, the detection frequency band is mainly distributed above 10 Hz. When the frequency is between 0.1 MHz and 1 Hz, it is necessary to use a gravitational wave observatory to detect gravitational waves in space, so as to minimize ground noise interference, to obtain higher detection sensitivity [2].

The detection of gravitational waves in space, such as the Laser Interferometer Space Antenna (LISA) and the Taiji Project, requires three spacecraft to form an equilateral triangle with an arm length of millions of kilometers [3,4]. These projects are designed to measure the propagation of laser light in a spacecraft, as shown in Figure 1. The laser light is

reflected by the test mass and then emitted through the beam expansion of the telescope. It is accepted in another spacecraft and the phase of the laser light is checked through the optical phase-locked loop, to detect gravitational waves existing in the universe through small changes in laser phase [5,6]. The accurate detection of gravitational waves requires an ultra-low measurement noise level, about 1 pm/$Hz^{1/2}$ in the low-frequency range from 0.1 mHz to 1 Hz [7]. To achieve this level of sensitivity, every component of a gravitational wave detector must meet stringent specifications. In fact, the normal operation of satellite payloads requires a very quiet environment, and there are many disturbances inside the spacecraft under orbital conditions [8–10]. The micro-vibration of the spacecraft caused by the in-orbit working state of the spacecraft reaction wheel assembly, gyroscope, etc., will also change the wavefront of the beam emitted or received by the telescope [11–13]. High-sensitivity precision equipment, such as micro-vibration in space gravitational wave detection, may not only have a resonance effect on the telescope structure, but also, as found in the analysis of this paper, low-frequency vibrations are directly coupled to the errors of gravitational wave measurements. High-frequency vibrations may even directly affect the phase demodulation accuracy of the optical phase-locked loop and have a more significant impact on the gravitational wave measurement.

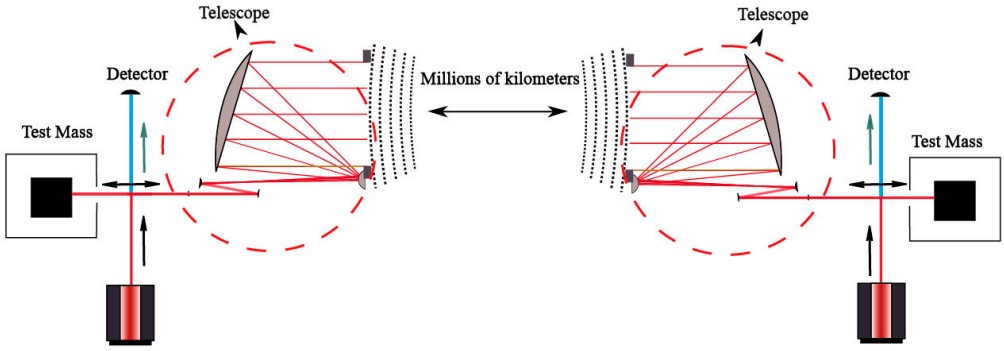

Figure 1. Schematic diagram of the far-field beam received by the gravitational wave telescope. The laser beam is expanded by the telescope and sent out to the detector after being received at the other end. The arrows in the figure indicate the direction of propagation of the beam.

The impact of vibration on interferometers has been analyzed in academia, such as the general analysis method of vibration on interferometers proposed by Peter J. de Groot et al. in the early stage. This method has strong adaptability but has different effects on specific scenarios [14,15]. Qian Liu et al. proposed a three-step iterative algorithm to suppress the sensitivity of phase-shift interferometry to mechanical vibrations [16]. The instantaneous interferometry proposed by R. Smythe et al. suppresses the vibration to a certain extent [17]. However, due to the particularity of the space gravitational wave measurement environment and the phase measurement method used, the above-mentioned theories and methods cannot successfully solve the influence of vibration on the gravitational wave measurement, so the establishment of a space gravitational wave detection environment to establish the coupling of vibration noise and optical path noise models is extremely necessary.

In this paper, we first introduce the two-beam interference model of space gravitational wave interference and the basic principle of OPLL (optical phase-locked loop), and then introduce the two-beam interference model by converting the vibration factor into the form of phase change, through Fourier analysis. The method reveals the influence of its vibration on the interference light intensity, and finally brings it into the working path of the phase-locked loop to obtain the coupling model of vibration and optical path. At the same time, in order to verify the correctness of the model, we conducted numerical and experimental simulation analyses, respectively. Finally, it was concluded that phase measurements are strongly affected by vibrations at specific frequencies as well as very low frequencies. Therefore, in engineering, we should avoid the coupling between the

low-frequency vibration and the space gravitational wave detection frequency band, and at the same time avoid the occurrence of the multiplication of the heterodyne frequency in the high frequency.

2. Vibration Coupling Model

2.1. Heterodyne Interference Model

In the gravitational wave detection interferometer, the far-field beam (according to the properties of Gaussian beams, the far-field beam can be approximated as a flat-top beam) is launched and propagated by the telescope beam expander system in the adjacent satellite. After the telescope intercepts and converges, it interferes with the local Gaussian laser on the quadrantal photodiode [18–21]. The space gravitational wave detection system is different from the ground gravitational wave detection. Due to the orbital drift, it is difficult for the two spacecraft to be absolutely stationary. Due to the relative motion, there must be a Doppler shift in the laser beam propagating from spacecraft A to spacecraft B, so the laser frequency changes. If we assume that the laser frequency when the laser is launched from spacecraft A is f_0, and the relative motion speed between the two spacecraft is ν, then the Doppler frequency shift generated by the laser reaching spacecraft B is $\Delta f = -\frac{v}{c} f_0$. Therefore, unlike the homodyne interferometry adopted by ground detection systems, space interferometry must adopt heterodyne interferometry. And, when we build the model, we use the method of heterodyne interference for derivation. For the convenience of research, we assume that the center position of the two beams is consistent with the incident angle. The final interference model can be written as follows:

$$\text{int} = \int_s E_{flat} E^*_{gauss} dr^2 = \int_s e^{-\frac{x^2+y^2}{w(z)^2}} e^{ik\Delta\varphi(\rho,\theta)} e^{i2\pi(f_1-f_2)t} dr^2 \tag{1}$$

where E_{flat} is the far-field beam, E_{gauss} is the local Gaussian beam, and f_1 and f_2 are the frequencies of the far-field and Gaussian beams, respectively. $w(z) = w_0\sqrt{1+(z/z_r)^2}$ is the beamwidth of the Gaussian beam, and $\Delta\varphi(\rho,\theta) = \varphi_2 - \varphi_1 - \frac{x^2+y^2}{2R(z)}$, where φ_1 and φ_2 are the initial phases of the local beam and the far-field beam, respectively. $R(z) = z(1+(\frac{z_r}{z})^2)$ is the radius of curvature of the equiphase surface of the Gaussian beam. It can be seen from the model that, when the spot size is small, the phase change $\Delta\varphi = \varphi_2 - \varphi_1$ caused by tiny vibrations is much larger than the waist width $w(z)$ and $\frac{x^2+y^2}{2R(z)}$ of the Gaussian beam, so in the subsequent analysis we simplify the model structure and write it as the light field form:

$$I = \overline{I}[1 + c\cos(\omega_{het} t + \varphi_0)] \tag{2}$$

where φ_0 is the initial phase including $\Delta\varphi$ and other forms, $\omega_{het} = 2\pi(f_2 - f_1)$ is the frequency of heterodyne interference, and $c = \frac{I_{max} - I_{\min}}{I_{max} + I_{\min}}$ is the contrast of the interference signal.

The form of micro-vibration is extremely complex. In order to analyze the influence of vibration on interference, we were inspired by Peter J. de Groot et al., and directly converted the vibration into the phase change in the interference signal. The formula is:

$$n(t) = 4\pi\frac{\delta L(t)}{\lambda} \tag{3}$$

where $\delta L(t)$ is the vibration form and λ is the wavelength of light. Then, we bring it into Formula (2) and we obtain the form of the light field affected by the vibration:

$$I' = \overline{I}[1 + c\cos(\omega_{het} t + \varphi_0 - n(t))] \tag{4}$$

For further analysis, we expand Formula (4):

$$I' = \overline{I} + \overline{I}c\{\cos(n(t))\cos(\omega_{het} t + \varphi_0) + \sin(n(t))\sin(\omega_{het} t + \varphi_0)\} \tag{5}$$

When the vibration amplitude is small, (5) can be simplified into the following formula:

$$\begin{cases} I' \approx I + \Delta I \\ \Delta I = \bar{I}cn(t)\sin(\omega_{het}t + \varphi_0) \end{cases} \tag{6}$$

Then, through Fourier transformation, we obtain:

$$\begin{cases} FT\{I'\} = FT\{I + \Delta I\} = FT\{I\} + FT\{\Delta I\} \\ FT\{\Delta I\} = -i\bar{I}c[N(v-f)e^{i\varphi_0} - N(v+f)e^{-i\varphi_0}]/2 \\ FT\{I\} = \bar{I}\delta(v) + \bar{I}c/2\{e^{i\varphi_0}\delta(v-f) + e^{-i\varphi_0}\delta(v+f)\} \end{cases} \tag{7}$$

where $N(v) = FT\{n(t)\}$ and f is the frequency of the heterodyne interference signal. After reorganizing, we finally obtain the model of vibration to interference light field:

$$\begin{aligned} FT\{I'\} = \bar{I}\delta(v) + \bar{I}c/2\{e^{i\varphi_0}[\delta(v-f) - iN(v-f)] \\ +e^{-i\varphi_0}[\delta(v+f) - iN(v+f)]\} \end{aligned} \tag{8}$$

From Formula (8), we understand that, under the premise of tiny vibration for the heterodyne interference signal, the frequency domain influence of the vibration phase factor $n(t)$ is concentrated on the two frequency bands of $v+f$ and $v-f$.

2.2. The Principle of Optical Phase-Locked Loop

In modern communication systems, there are many methods for digital phase modulation, including square loop, decision feedback method, and Costas method [22]. Among them, the Costas Loop can effectively track the suppressed carrier signal with low signal-to-noise ratio, has excellent performance, and consumes fewer hardware resources, so it is used in many units in space gravitational wave detection [23]. As shown in Figure 2, it consists of a local numerically controlled oscillator (NCO), a multiplier, a low-pass filter (LPF), and a loop controller.

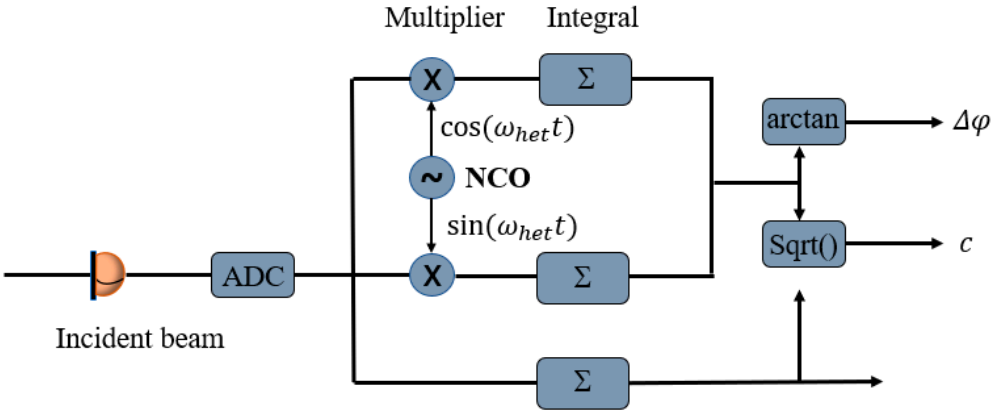

Figure 2. Schematic diagram of Costas Loop demodulation algorithm. The incident light is converted into an electrical signal via a phase meter, and the NCO sends out a heterodyne frequency signal and multiplies and integrates the interference signal to obtain a phase signal.

Its working principle can be divided into the following steps:

1. After the incident light enters the Costas Loop, the optical signal is converted into an electrical signal.
2. The sine and cosine signals are multiplied by the incident signal through the NCO (numerical oscillator). Although in actual detection, the heterodyne frequency is unknown due to the existence of the Doppler effect, there is a subsequent feedback mechanism so that the final NCO emits the same sine–cosine signal as the heterodyne frequency. However, for the convenience of this research, the feedback processing pro-

cess has nothing to do with phase demodulation, and we assume that the heterodyne frequency is known. Then, we obtain:

$$\begin{array}{l} S = \int_0^{2\pi} \cos(\omega_{het}t) \cdot I(\omega_{het}t) d(\omega_{het}t) = \overline{I} c\pi \cos(\Delta\varphi) \\ C = \int_0^{2\pi} \sin(\omega_{het}t) \cdot I(\omega_{het}t) d(\omega_{het}t) = \overline{I} c\pi \sin(\Delta\varphi) \end{array} \tag{9}$$

(3) When the frequency of the NCO is consistent with the heterodyne frequency, we obtain the phase formula of the beam:

$$\Delta\varphi = -\frac{S}{C} \tag{10}$$

2.3. The Influence of Micro-Vibration on Phase Demodulation

In order to analyze the influence of vibration on phase demodulation, we substitute $\Delta I = \overline{I} cn(t) \sin(\omega_{het}t + \varphi_0)$ in (6) into (9). We obtain the change of the OPLL analysis results caused by vibration and noise:

$$\begin{array}{rl} \Delta S & = \int_0^{\frac{2\pi}{\omega_{het}}} \cos(\omega_{het}t) \cdot \Delta I(\omega_{het}t) dt \\ & = \int_{-\infty}^{+\infty} FT\{\cos(\omega_{het}t)\} * \cdot FT\{\Delta I(\omega_{het}t)\} dv \\ & = \frac{1}{2}\int_{-\infty}^{+\infty} [\delta(v-f) + \delta(v+f)] \cdot FT\{\Delta I\} dv \\ & = -\frac{ic\overline{I}}{4}\int_{-\infty}^{+\infty} [\delta(v-f) + \delta(v+f)] \cdot [N(v-f)e^{i\varphi_0} - N(v+f)e^{-i\varphi_0}] dv \\ & = -\frac{ic\overline{I}}{4}\{[N(0)e^{i\varphi_0} - N(2f)e^{-i\varphi_0}] + [N(-2f)e^{i\varphi_0} - N(0)e^{-i\varphi_0}]\} \end{array} \tag{11}$$

and

$$\begin{array}{rl} \Delta C & = \int_0^{\frac{2\pi}{\omega_{het}}} \sin(\omega_{het}t) \cdot \Delta I(\omega_{het}t) dt \\ & = \int_{-\infty}^{+\infty} FT\{\sin(\omega_{het}t)\} * \cdot FT\{\Delta I(\omega_{het}t)\} dv \\ & = \frac{i}{2}\int_{-\infty}^{+\infty} [\delta(v-f) - \delta(v+f)] \cdot FT\{\Delta I\} dv \\ & = \frac{c\overline{I}}{4}\int_{-\infty}^{+\infty} [\delta(v-f) + \delta(v+f)] \cdot [N(v-f)e^{i\varphi_0} - N(v+f)e^{-i\varphi_0}] dv \\ & = \frac{c\overline{I}}{4}\{[N(0)e^{i\varphi_0} - N(2f)e^{-i\varphi_0}] + [N(-2f)e^{i\varphi_0} - N(0)e^{-i\varphi_0}]\} \end{array} \tag{12}$$

For writing convenience, we rewrite (10) as $\varphi_0 = \arctan\left[\frac{S}{C}\right]$, and if we differentiate it, we obtain the gradient formula of φ_0:

$$\begin{array}{rl} \Delta\varphi_0 & \approx \Delta S \frac{d\varphi_0}{dS} + \Delta C \frac{d\varphi_0}{dC} \\ & = \Delta S \frac{C}{S^2+C^2} - \Delta C \frac{S}{S^2+C^2} \\ & = \frac{2f}{\overline{I}c\pi}[\Delta S \cos(\varphi_0) - \Delta C \sin(\varphi_0)] \end{array} \tag{13}$$

Finally, we substitute (11) and (12) into (13) to obtain the final model:

$$\begin{array}{rl} \Delta\varphi_0 & = \frac{f}{2\pi}\{[N(0)e^{i\varphi_0} - N(2f)e^{-i\varphi_0}] \\ & + [N(-2f)e^{i\varphi_0} - N(0)e^{-i\varphi_0}]\} \cdot [-i\cos(\varphi_0) - \sin(\varphi_0)] \end{array} \tag{14}$$

This result shows that, in the detection of gravitational waves in space, tiny vibrations are coupled into the two-beam interference model and have an impact on the phase analysis results of the subsequent OPLL. Its phase measurement error $\Delta\varphi_0$ is related to the frequency f of heterodyne interference, the initial phase φ_0, and the Fourier change of the vibration factor $N(v)$. It is worth noting that, since the structure of the Costas Loop itself has filtered out the influence of the vibration noise of most frequencies on the phase, only $N(-2f)$, $N(0)$, and $N(2f)$ still have an influence. Therefore, if the double-frequency vibration noise

of the heterodyne frequency and the DC vibration noise can be filtered out, the influence of micro-vibration on the phase measurement can be greatly reduced.

3. Numerical Simulation

Through the establishment of the coupling model of vibration noise and optical path noise above, we reveal how vibration noise affects the phase measurement in gravitational wave detection. In order to better verify the accuracy of the model, we next use numerical simulation to conduct experiments according to the relevant parameters of the detector and beam. First, we construct a Gaussian beam and a flat-hat beam with a wavelength of 1064 nm, and the beam propagation distance is 0.5 m. Then, we use a quadrantal photodiode to detect the heterodyne interference signal [24]. Its structure is shown in Figure 3; its radius l is 2.5 mm, slit width is 1 um, and the heterodyne frequency f is 1 MHz. The sampling time of the optical phase-locked loop is 10^{-5} s, which can complete the integration of the heterodyne interference signal in multiple cycles. Finally, we couple 20 kinds of vibration noise with amplitude 10^{-12} m and frequency $0.1f \sim 2f$ into the interference model, and the phase measurement is completed within 100 sampling times. The results are shown in Figure 4.

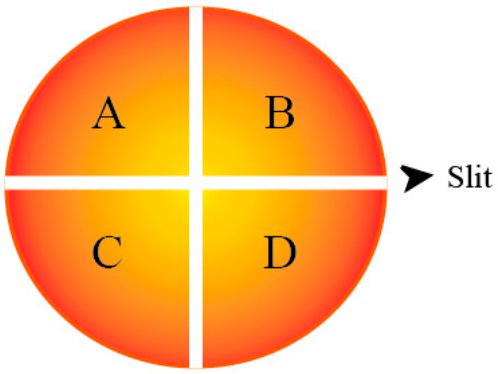

Figure 3. Schematic diagram of the principle of QPD, which is composed of A–D four photoelectric detectors, and the width of each connected slit is about 1 um.

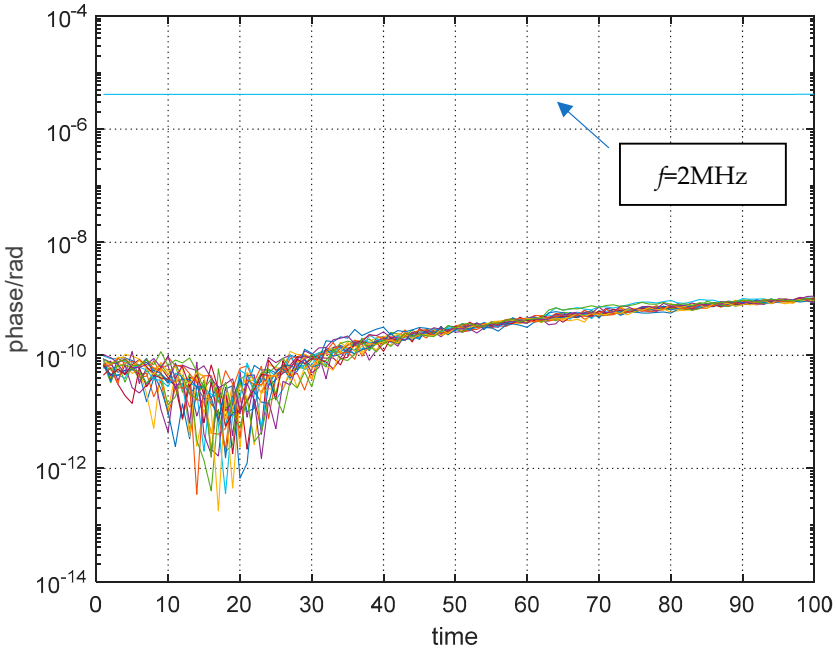

Figure 4. The amplitude is 10^{-12} m, and the frequency distribution is between $0.1f$ and $2f$. The phase noise generated by 20 kinds of vibration noise.

These results show that, under the premise of tiny vibrations, the phase noises produced by vibration noises of different frequencies are different in gravitational wave detection. Especially when the vibration noise frequency reaches the multiplier of the heterodyne frequency, its influence is most obvious. From a numerical point of view, the phase noise generated by frequency multiplication noise is about 4.12×10^{-6} rad; converting this to optical path noise is about 6.98×10^{-13} m. This value is close to the amplitude of the input vibration noise, while the vibration noise of other frequencies is much lower than this value, indicating that most of the vibration noise is isolated by the phase-locked loop, but the multiplier part is retained.

In addition, we simulated the performance of phase error and optical path error under different amplitudes. It can be seen from Table 1 that, when the amplitude is small, the impact of vibration noise of double frequency is very prominent compared with the vibration noise of other frequencies, and the optical path noise caused by it is almost the same as its amplitude. This shows that the influence of double-frequency noise is coupled into the OPLL in a manner similar to the magnitude of the direct current of its amplitude, which causes significant interference to the accuracy of space gravitational wave detection, so we should try to avoid it in engineering.

Table 1. Phase and optical path noise caused by vibration noise in different frequency bands.

Amplitude (m)	f =2 MHz		f ≠ 2 MHz	
	Phase (Rad)	Optical Path (m)	Phase (Rad)	Optical Path (m)
10^{-12}	4.12045×10^{-6}	6.98114×10^{-13}	-3.5877×10^{-10}	-6.07852×10^{-17}
10^{-11}	4.12029×10^{-5}	6.98087×10^{-12}	-3.5306×10^{-9}	-5.98178×10^{-16}
10^{-10}	4.11873×10^{-4}	6.97823×10^{-11}	-2.9720×10^{-8}	-5.03536×10^{-15}
10^{-9}	4.10321×10^{-3}	6.95194×10^{-10}	2.6232×10^{-7}	4.44440×10^{-14}
10^{-8}	3.95824×10^{-2}	6.70632×10^{-9}	5.8774×10^{-5}	9.95789×10^{-12}
10^{-7}	0.321447	5.44617×10^{-8}	0.0093	1.57567×10^{-9}
10^{-6}	−0.443667	-7.51691×10^{-8}	−0.3666	-6.21118×10^{-8}

At the same time, we additionally analyzed the performance of vibration and noise in the detection frequency band of space gravitational waves. We also use the above-mentioned numerical analysis method to substitute the vibration noise with frequencies of 0.1 MHz, 1 MHz, 10 MHz, 100 MHz, and 1 Hz into the above model for analysis. The results are shown in Figure 5 below:

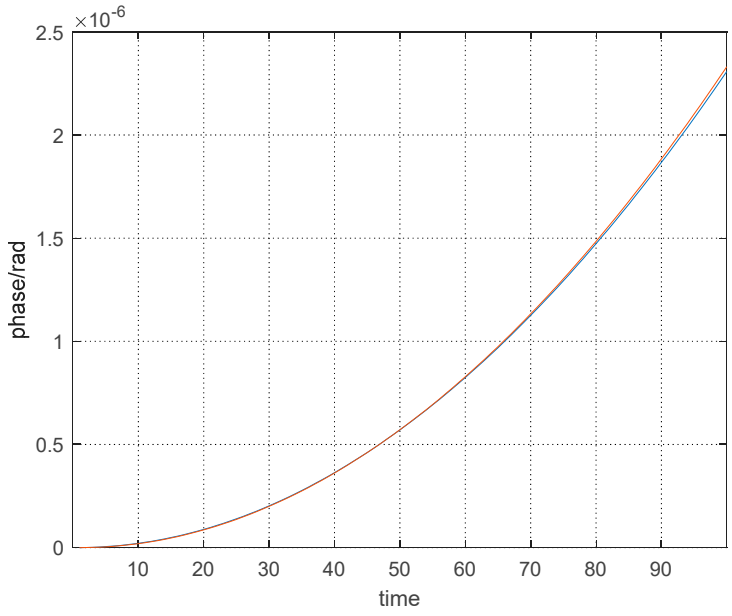

Figure 5. Influence of vibration noise in the test frequency band of gravitational waves in space on

the phase measurement. The red line is the phase effect brought on by the vibration noise of 0.1 MHz, 1 MHz, 10 MHz, 100 MHz, and 1 Hz. They almost overlap; the blue line is the time distribution of the vibration noise itself.

This conclusion shows that, under the premise of tiny vibration, when the frequency of the vibration noise is much lower than the frequency of the heterodyne interference signal, the phase effect generated by the vibration noise is almost consistent with its own form. Therefore, it shows that the low-frequency noise appears as a DC flow in the Costas Loop, and for the space gravitational wave detection, in order to avoid its interference with the gravitational wave signal, it also needs to be suppressed.

4. Simulation

In order to verify the above conclusions, our experimental setup is shown in Figure 6 below, which includes three parts: signal generation circuit, phase-locked loop circuit, and PC. In this experiment, the signal parameters are sent to the signal generation circuit through the PC to generate the laser heterodyne interference analog signal coupled with vibration noise, and then the signal is connected to the phase-locked loop circuit, and the phase data port is connected to the PC for real-time analysis and recording.

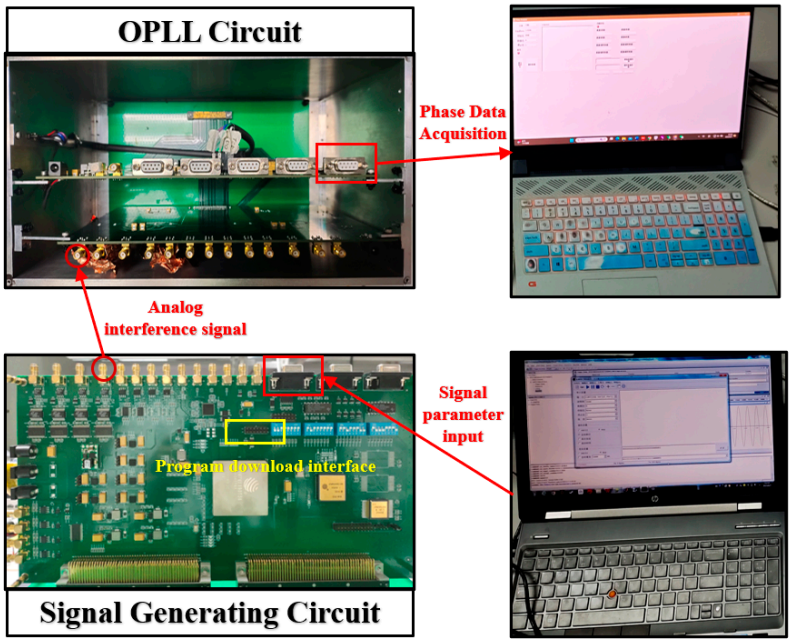

Figure 6. Experimental diagram. PC1 inputs the signal parameters into the signal generation circuit to generate an analog interference signal, and then sends the signal to the OPLL circuit, and PC2 analyzes and receives the phase signal in real time.

The algorithms in this experiment are all based on the FPGA (Field Programmable Gate Array) platform, and its model is XC7K325T-2FFG900I in the K7 series. This type of FPGA has 900 input and output pins, 203,800 lookup table resources, and 407,600 flip-flop resources, etc., which can meet the resources required for computing. There are digital interfaces on the board for communication, the main interfaces include DB9 and SMA, the frequency and noise multiplier set by the signal are sent from the PC to the FPGA through the DB9 to USB cable, and the generated signal is output through the SMA port. The board is designed with a highly stable crystal oscillator to provide a clock reference for the FPGA. The crystal oscillator model is SCO-533350-80M, which can generate a clock of 80 MHz to meet the requirements of signal sampling. In addition, the FPGA is externally connected with a DAC module LTC1668 chip to convert the 16-bit digital signal output by the FPGA into an analog voltage signal.

The signal generation algorithm in this paper is realized based on VHDL language. The algorithm is divided into four modules according to the design modules, as shown in Figure 7. They are, respectively, a communication module, a data analysis module, a clock module, and a signal generation module. The PC sends the signal parameters through the RS232 serial port protocol, which are the frequency increment word corresponding to the signal frequency, the frequency increment word corresponding to the coupled noise frequency, and the hexadecimal number of the noise multiplier. Three parameters are accepted in the communication module and obtained in the data-unpacking module. According to the three signal parameters, the signal generation module first calculates the noise figure through the multiplier and generates the vibration noise signal based on the principle of DDS (Direct Digital Synthesis). Secondly, the real-time phase of the vibration noise is calculated by the multiplier; based on the DDS principle again, the real-time phase of the vibration noise is used as the phase item, and the frequency of the signal is used as the frequency item to generate a sinusoidal signal coupled with the vibration noise. Finally, according to the DA output requirements, the sinusoidal signal is converted into data, and the analog voltage signal is output.

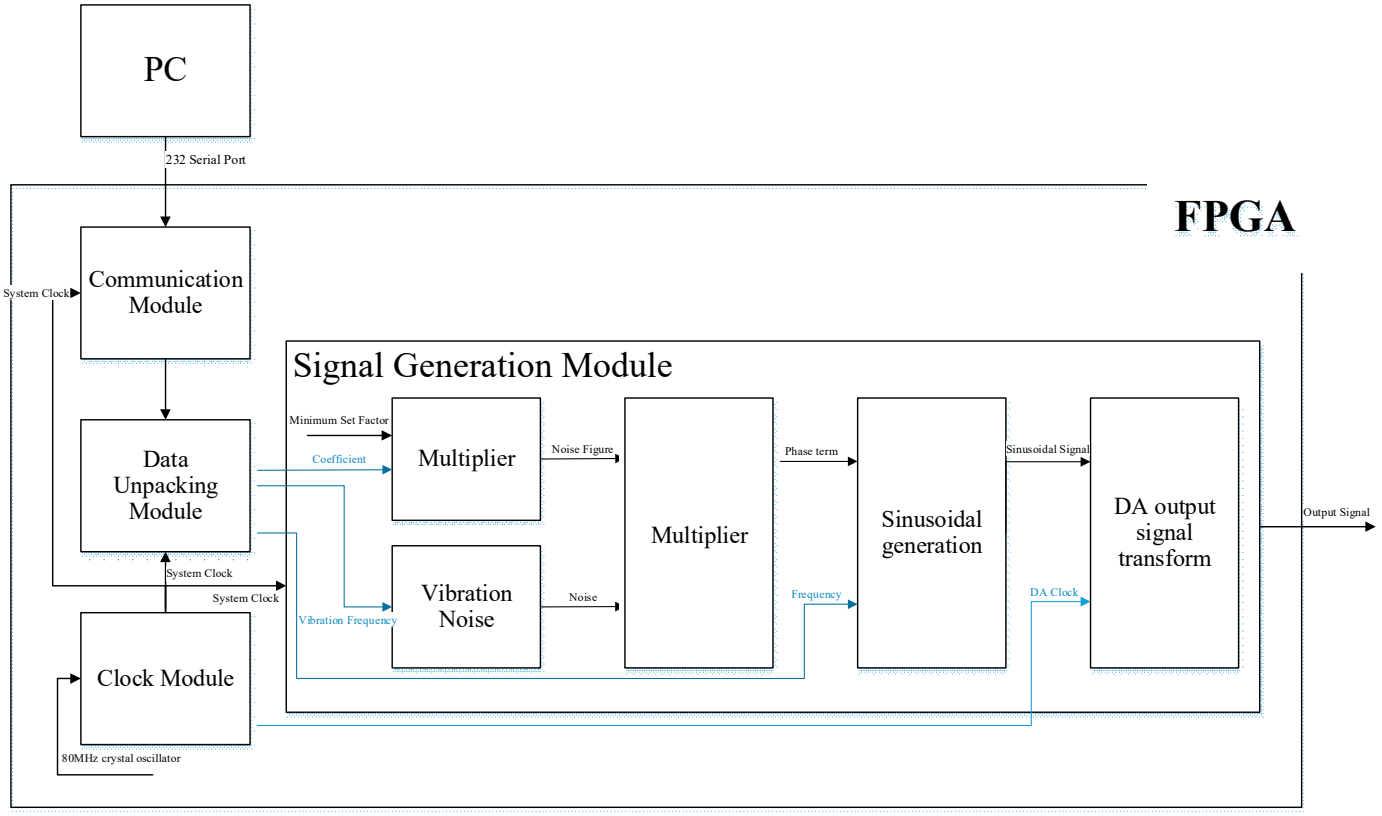

Figure 7. Schematic diagram of signal generation algorithm.

After completing the construction of the above experimental device, we set the vibration noise with an amplitude of 10–12 m and a frequency of $0.1f \sim 4f$ and coupled it into the heterodyne interference signal. Then, we used the phase meter to analyze and record the real-time phase of the signal on the PC. As shown in Figure 8, after removing the initial phase, we obtained the phase change data within 300 s. The upper part is the phase change caused by f $\neq$ 2 MHz vibration noise (random distribution of noise at different frequencies), and the lower part is f = 2 MHz. It is obvious that, although the electronic noise of the experimental system itself has not been completely suppressed, the distribution of the data is different from that in Figure 4, and the noise distribution is relatively scattered, but in terms of overall performance, it still follows the above-mentioned theory. In conclusion,

the influence of double-frequency noise is much greater than that of other frequencies, and so this experiment effectively proves the correctness of the theory in this article.

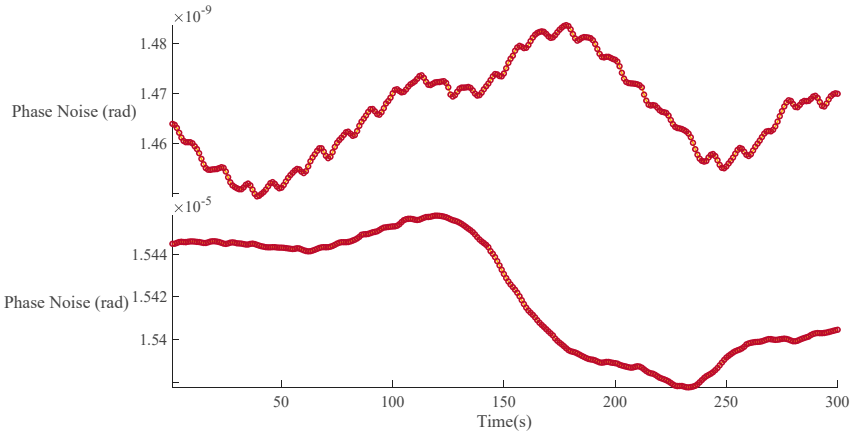

Figure 8. Experimental results diagram, the upper part is f $\neq$ 2 MHz and the lower part is f = 2 MHz.

5. Discussion

The essence of space gravitational wave detection lies in the utilization of stellar interferometry principles using laser interferometry to measure the relative distance changes between satellites, thereby inferring gravitational wave signals. However, in the case of spacecraft operating in orbit, certain internal components introduce small vibrations characterized by complex vibration patterns and a wide frequency distribution. Currently, both the LISA mission and the "Taiji Project" only consider the impact of telescope vibrations to avoid resonance effects, largely neglecting vibration suppression at most frequencies. This poses a critical issue that needs to be addressed in the context of space gravitational wave detection.

In this paper, we first establish a model for dual-beam heterodyne interferometry. By analyzing and simplifying the model, we derive an intensity-based interferometric model. We then incorporate the vibration model into the interferometric model as a phase modulation factor, leading to the conclusion that vibration noise at specific frequencies couples into the phase information of the heterodyne interferometry model. Next, we introduce the principle of OPLL and construct an OPLL model. The coupled optical signal mentioned above is input into the OPLL model. Finally, we obtain a noise-coupling model for space gravitational wave measurements. The model indicates that the phase error is related to both the DC component and the component at a frequency of $2f$ of the vibration factor, where f represents the frequency of the heterodyne signal.

In terms of experimental proof, we carried out a numerical simulation analysis and an experimental analysis, respectively, and conducted a comprehensive analysis on the vibration noise of most video frequencies on average, and finally showed that the results are consistent with the theoretical basis. When the amplitude is less than 10^{-8} m, the large optical path error caused by the frequency is close to its amplitude, while the optical path difference caused by other frequencies is much smaller than the amplitude.

In summary, the influence of small vibrations generated internally by spacecraft in orbit on space gravitational wave measurements is inevitable. We need to consider not only the resonance effects on the telescope structure and the potential damage to structural materials, but also the suppression of interference from vibrations at specific frequencies. This has significant implications for the optical and mechanical design of missions like LISA or the Taiji Project.

Author Contributions: Conceptualization, Z.C.; methodology, Z.C.; software, Z.C. and Z.W. (Zhenpeng Wang); validation, Z.C.; formal analysis, Z.C.; investigation, Z.C.; writing—original draft preparation, Z.C.; writing—review and editing, Z.W. (Zhi Wang) and C.F.; visualization, Z.W. (Zhi Wang); resources, Z.W. (Zhi Wang); supervision, C.Y., Z.W. (Zhi Wang) and C.F.; funding acqui-

sition, Z.W. (Zhi Wang) and C.F. All authors have read and agreed to the published version of the manuscript.

Funding: This research was funded by the National Natural Science Foundation of China, grant number 62075214 and the National Key R&D Program of China, grant number 2020YFC2200104.

Data Availability Statement: The data and the source code are publicly available on https://github.com/DrChenZW/Photonic.git (accessed on 13 June 2023).

Conflicts of Interest: The authors declare no conflict of interest.

References

1. Bian, L.; Cai, R.-G.; Cao, S.; Cao, Z.; Gao, H.; Guo, Z.-K.; Lee, K.; Li, D.; Liu, J.; Lu, Y. The gravitational-wave physics II: Progress. *Sci. China Phys. Mech. Astron.* **2021**, *64*, 120401. [CrossRef]
2. Zheng, K.; Xu, M. Design and Thermal Stability Analysis of Swing Micro-Mirror Structure for Gravitational Wave Observatory in Space. *Machines* **2021**, *9*, 104. [CrossRef]
3. Jennrich, O. LISA technology and instrumentation. *Class. Quantum Gravity* **2009**, *26*, 153001. [CrossRef]
4. Chen, Z.; Leng, R.; Yan, C.; Fang, C.; Wang, Z. Analysis of Telescope Wavefront Aberration and Optical Path Stability in Space Gravitational Wave Detection. *Appl. Sci.* **2022**, *12*, 12697. [CrossRef]
5. Dong, Y.; Liu, H.; Luo, Z.; Li, Y.; Jin, G. A comprehensive simulation of weak-light phase-locking for space-borne gravitational wave antenna. *Sci. China Technol. Sci.* **2016**, *59*, 730–737. [CrossRef]
6. Luo, Z.; Guo, Z.; Jin, G.; Wu, Y.; Hu, W. A brief analysis to Taiji: Science and technology. *Results Phys.* **2020**, *16*, 102918. [CrossRef]
7. Wang, Z.; Yu, T.; Zhao, Y.; Luo, Z.; Sha, W.; Fang, C.; Wang, Y.; Wang, S.; Qi, K.; Wang, Y.; et al. Research on Telescope TTL Coupling Noise in Intersatellite Laser Interferometry. *Photonic Sens.* **2019**, *10*, 265–274. [CrossRef]
8. Zhang, L.; Wang, W.; Shi, Y. Development of a magnetorheological damper of the micro-vibration using fuzzy PID algorithm. *Arab. J. Sci. Eng.* **2019**, *44*, 2763–2773. [CrossRef]
9. Zhou, W.; Li, D. Experimental research on a vibration isolation platform for momentum wheel assembly. *J. Sound Vib.* **2013**, *332*, 1157–1171. [CrossRef]
10. Yu, Y.; Gong, X.; Zhang, L.; Jia, H.; Xuan, M. Full-Closed-Loop Time-Domain Integrated Modeling Method of Optical Satellite Flywheel Micro-Vibration. *Appl. Sci.* **2021**, *11*, 1328. [CrossRef]
11. Wang, H.; Wang, W.; Wang, X.; Zou, G.-y.; Li, G.; Fan, X. Space camera image degradation induced by satellite micro-vibration. *Acta Photon. Sin.* **2013**, *42*, 1212–1217. [CrossRef]
12. Pang, S.-W.; Yang, L.; Qu, G. New development of micro-vibration integrated modeling and assessment technology for high performance spacecraft. *Struct. Environ. Eng.* **2007**, *34*, 1–9.
13. Jiao, X.; Zhang, J.; Li, W.; Wang, Y.; Ma, W.; Zhao, Y. Advances in spacecraft micro-vibration suppression methods. *Prog. Aerosp. Sci.* **2023**, *138*, 100898. [CrossRef]
14. De Groot, P.J. Vibration in phase-shifting interferometry. *JOSA A* **1995**, *12*, 354–365. [CrossRef]
15. Deck, L.L. Suppressing phase errors from vibration in phase-shifting interferometry. *Appl. Opt.* **2009**, *48*, 3948–3960. [CrossRef] [PubMed]
16. Liu, Q.; Wang, Y.; He, J.; Ji, F. Modified three-step iterative algorithm for phase-shifting interferometry in the presence of vibration. *Appl. Opt.* **2015**, *54*, 5833–5841. [CrossRef] [PubMed]
17. Smythe, R.; Moore, R. Instantaneous phase measuring interferometry. *Opt. Eng.* **1984**, *23*, 361–364. [CrossRef]
18. Zhao, Y.; Shen, J.; Fang, C.; Liu, H.; Wang, Z.; Luo, Z. Tilt-to-length noise coupled by wavefront errors in the interfering beams for the space measurement of gravitational waves. *Opt. Express* **2020**, *28*, 25545–25561. [CrossRef]
19. Zhao, Y.; Shen, J.; Fang, C.; Wang, Z.; Gao, R.; Sha, W. Far-field optical path noise coupled with the pointing jitter in the space measurement of gravitational waves. *Appl. Opt.* **2021**, *60*, 438–444. [CrossRef]
20. Zhao, Y.; Wang, Z.; Li, Y.; Fang, C.; Liu, H.; Gao, H. Method to Remove Tilt-to-Length Coupling Caused by Interference of Flat-Top Beam and Gaussian Beam. *Appl. Sci.* **2019**, *9*, 4112. [CrossRef]
21. Sasso, C.P.; Mana, G.; Mottini, S. Coupling of wavefront errors and jitter in the LISA interferometer: Far-field propagation. *Class. Quantum Gravity* **2018**, *35*, 185013. [CrossRef]
22. Han, S.; Tong, J.; Wang, Z.; Yu, T.; Sui, Y. Simulation system of a laser heterodyne interference signal for space gravitational wave detection. *Infrared Laser Eng.* **2022**, *51*, 20210572.
23. Wang, Z.; Yu, T.; Sui, Y.; Wang, Z. Beat-Notes Acquisition of Laser Heterodyne Interference Signal for Space Gravitational Wave Detection. *Sensors* **2023**, *23*, 3124. [CrossRef]
24. Meshksar, N.; Mehmet, M.; Isleif, K.S.; Heinzel, G. Applying Differential Wave-Front Sensing and Differential Power Sensing for Simultaneous Precise and Wide-Range Test-Mass Rotation Measurements. *Sensors* **2020**, *21*, 164. [CrossRef] [PubMed]

Disclaimer/Publisher's Note: The statements, opinions and data contained in all publications are solely those of the individual author(s) and contributor(s) and not of MDPI and/or the editor(s). MDPI and/or the editor(s) disclaim responsibility for any injury to people or property resulting from any ideas, methods, instructions or products referred to in the content.